Cr(II) and Cr(I) PCP Pincer Complexes: Synthesis, Structure, and Catalytic Reactivity

Daniel Himmelbauer,[†] Berthold Stöger,[‡] Luis F. Veiros,[≠] Marc Pignitter,[§] and Karl Kirchner*, [†]

[†] Institute of Applied Synthetic Chemistry, Vienna University of Technology, Getreidemarkt 9, A-1060 Vienna, AUSTRIA

[‡] X-Ray Center, Vienna University of Technology, Getreidemarkt 9, A-1060 Vienna, AUSTRIA

[≠] Centro de Química Estrutural, Instituto Superior Técnico, Universidade de Lisboa, Av. Rovisco Pais No. 1, 1049-001 Lisboa, PORTUGAL

[§] Department of Physiological Chemistry, Faculty of Chemistry, University of Vienna, Althanstrasse 14, 1090 Vienna, AUSTRIA

ABSTRACT: In the current investigation, the reaction of $[Cr(CO)_6]$ with the ligand precursor PO(C-Br)OP-tBu (**1**) was investigated. When a suspension of $[Cr(CO)_6]$ and **1** in toluene was transferred into a sealed microwave glass vial and stirred for 3 h at 180 °C the square-planar Cr(II) complex [Cr(POCOP-tBu)Br] (**2**) was obtained. Treatment of **2** with 1 equiv of Li[HBEt$_3$] in THF led to the formation of the borohydride complex [Cr(POCOP-tBu)(κ^2-BH$_4$)] (**3**). Exposure of a toluene solution of **3** to NO gas (1 bar) at room temperature affords the Cr(I) complex [Cr(POCOP-tBu)(NO)(κ^2-BH$_4$)] (**4**). Alternatively, **4** was also obtained by reacting [Cr(POCOP-tBu)(NO)(Br)] (**5**) with Li[HBEt$_3$]. Based on magnetic and EPR measurements as well as DFT calculations, compounds **4** and **5** adopt a low-spin d^5 configuration and feature a nearly linear bound NO ligand

suggesting Cr^{I}NO$^+$ rather than Cr^{II}NO$^\bullet$ character. The reaction of **2** with 1 equiv of LiCH$_2$SiMe$_3$ in toluene afforded the square planar alkyl complex [Cr(POCOP-tBu)(CH$_2$SiMe$_3$)] (**6**) in 57% yield. This compound is catalytically active for the hydrosilylation of ketones at room temperature with a catalyst loading of 0.5 mol%. X-ray structures of all complexes are presented.
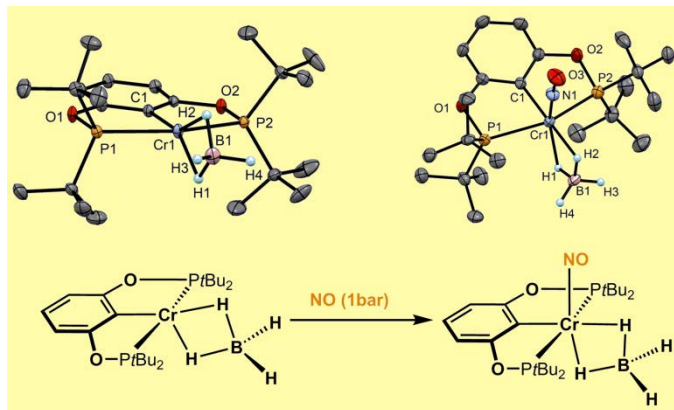
INTRODUCTION

PCP pincer ligands[1] where phosphine donors are connected *via* CH$_2$, O, or NR spacers to an aromatic benzene backbone in the two ortho positions have become extremely valuable scaffolds for the stabilization and activation of transition metal fragments.[2] These type of ligands can be rationally designed in a modular fashion and permits the preparation of highly active catalysts for a large variety of chemical reactions which proceed with high efficiency and selectivity.[2] With respect to first-row transition metals, the chemistry of nickel PCP complexes is already quite comprehensive, studies of cobalt, iron and manganese PCP pincer complexes is exceedingly rare or virtually non-existing such as in the case of chromium.[2p] This may be attributed to the failure of many simple metal salts to cleave the C-H bonds of the arene moiety of the pincer ligands and/or the thermodynamic instability of the resulting hydride complexes.[3,4] Instead of a directed intramolecular cyclometallation of the *ipso* C-H bond, we utilize here the oxidative addition PO(C-Br)OP-tBu (**1**) to the Cr(0) complex $[Cr(CO)_6]$ as synthetic approach for the synthesis of the square-planar Cr(II) PCP complex [Cr(POCOP-tBu)(Br)] (**2**) which is a valuable precursor for novel chromium borohydride PCP pincer complexes in formal oxidation states +I and +II. X-ray structures of representative complexes are presented.

RESULTS AND DISCUSSION

When a suspension of $[Cr(CO)_6]$ and PO(C-Br)OP-tBu (**1**) in toluene was placed in a sealed microwave glass vial and stirred for 3 h at 180 °C, after workup, the analytically pure 12e complex [Cr(POCOP-tBu)(Br)] (**2**) was obtained in 76% isolated yield (Scheme 1). As judged by solution magnetic susceptibility measurements (CD$_2$Cl$_2$, Evans method), this compound is a high-spin complex with a olution effective magnetic moment of 4.8(4) μ$_B$. This is in agreement with a high-spin d^4 center (four unpaired electron) and is thus in the same range as the theoretical spin-only value of 4.90 μ$_B$.

1

The solid-state structure of **2** was established by single-crystal X-ray crystallography. A molecular view is depicted in Figure 1 with selected bond distances given in the captions. The molecular structure shows the metal in a typical distorted-square planar configuration. The C1-Cr1-Br1 angle deviates slightly from linearity being 178.68(6)°. The P(1)-Cr1-P2 angle is 154.08(1)°. The Cr-C_{ipso} bond distance of 2.084(3) Å is comparable to those of other Cr(II) aryl complexes.[5]

Scheme 1. Synthesis of Complex 2
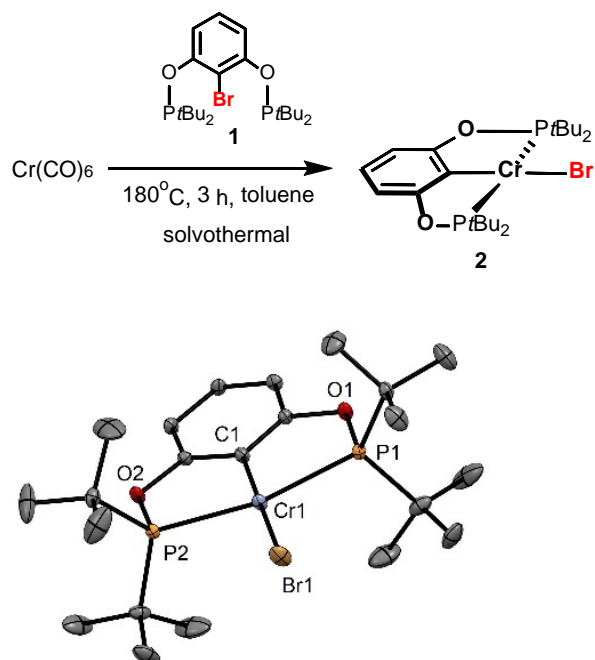
Figure 1. Structural view of [Cr(POCOP-*t*Bu)(Br)] (**2**) showing 50% thermal ellipsoids (H atoms omitted for clarity). Selected bond lengths (Å) and bond angles (°): Cr1-C1 2.084(3), Cr1-Br1 2.4527(7), Cr1-P1 2.457(1), Cr1-P2 2.457(1), P1-Cr1-P2 154.08(3), C1-Cr1-Br1 178.68(6).

Treatment of **2** with 2 equiv of LiBH$_4$ in THF for 24 h afforded the borohydride complex [Cr(POCOP-*t*Bu)(κ^2-BH$_4$)] (**3**) in 86% yield as black solid (Scheme 2). Based on EPR (see SI) and solution magnetic susceptibility measurements (CD$_2$Cl$_2$, Evans method), **3** is also a d^4-high-spin complex with a solution effective magnetic moment of 4.9(4) μ_B. The κ^2-coordination mode of BH$_4^-$ ligand was first established by IR spectroscopy. Attenuated total reflectance IR spectra of the solid samples of **3** exhibit strong bands at 2407 and 2068 cm^{-1} which are attributed to the terminal and bridging hydrogen-boron stretches ν_{B-Ht} and ν_{B-Hb}, respectively.

Scheme 2. Synthesis of Complexes 3 and 4
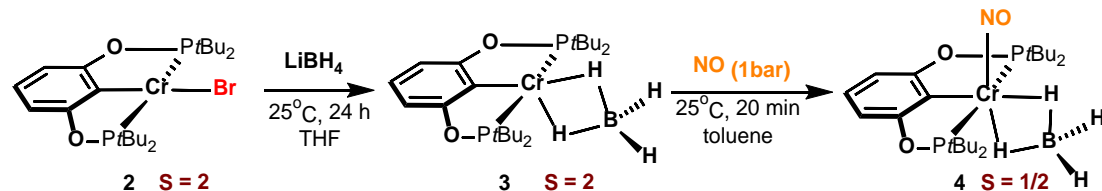
The electronic structure of complex **3** was studied by means of DFT calculations. The calculated spin density is essentially centered on the metal and the frontier orbitals (*d*-splitting) are the expected ones for a pseudo-trigonal bipyramid d^4 high spin complex,[6] as shown in Figure 2. The bonding and charge distribution are also in agreement with a Cr(II) complex, with a clearly positive charge on the metal atom (C = 0.58), while ligand donation is reflected by the ligand charges of C(PCP) = 0.11 and C(BH$_4$) = -0.69. The coordination of the BH$_4^-$ ligand derives from two B–H σ-donations resulting in a weakening of the coordinated B–H bonds when compared with the free ones, as shown by the corresponding Wiberg indices (WI)[7] being 0.84 and 0.97, respectively. Interestingly, the coordination of BH$_4^-$ is symmetric with two equivalent Cr-H bonds (WI = 0.10).

The solid-state structure of **3** was determined by X-ray diffraction unequivocally establishing the κ^2-bonding mode of the BH$_4^-$ ligand. A structural view is presented in Figure 3 with selected metrical parameters given in the caption. Chromium

borohydride complexes are exceedingly rare and only a few species such as [CrCp(κ^2-BH$_4$)] and [Cr(κ^2-BH$_4$)$_2$(THF)$_2$] have been reported but were characterized merely on the basis of their spectroscopic and microanalytical data.[8,9] Only in the case of [Cr(κ^2-BH$_4$)(H)(dmpe)$_2$][10] and [Cr(TMEDA)(κ^2-BH$_4$)$_2$][11] a complete structural analysis was provided. There is as yet no report of chromium borohydride pincer complexes.
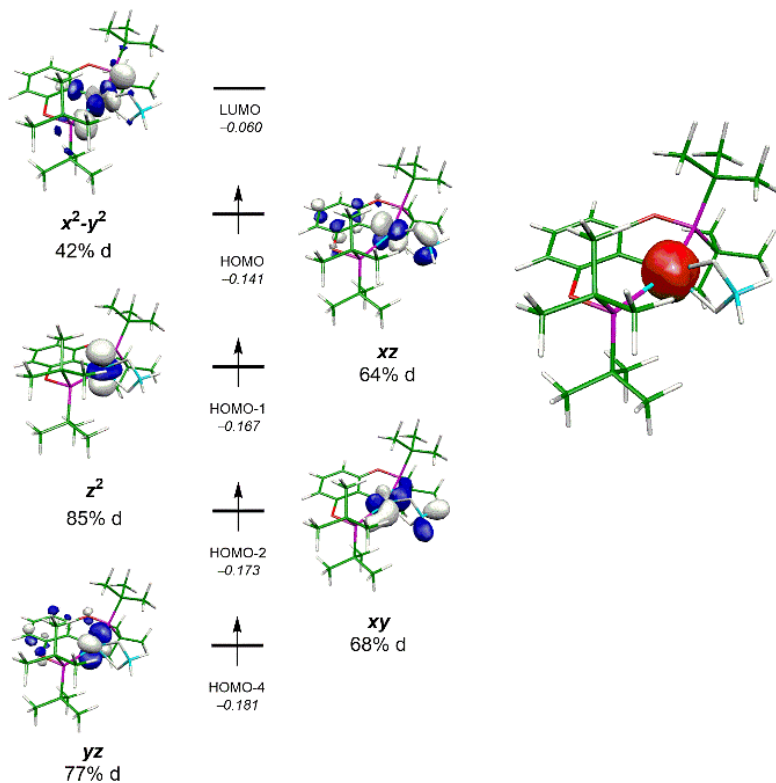

Figure 2. Frontier orbitals (*d*-splitting) and spin density for [Cr(POCOP-*t*Bu)(κ^2-BH$_4$)] (**3**). Orbital energy values in hartrees (italics).

The metal center is in a five-fold coordination by one C, two P and two H atoms furnished by the κ^3-*P,C,P*-bonded pincer ligand and by the κ^2-bonded BH$_4^-$ anion, respectively. The coordination sphere of the chromium can be described as a distorted trigonal bipyramid with C1, H1, and H2 in the equatorial position and P1 and P2 as the axial atoms. The positions of the bridging and terminal hydrides H$_b$ and H$_t$ of the BH$_4^-$ ligand could be located in the difference Fourier map and refined isotropically. From this Cr1-H1 and Cr1-H2 distances of 1.91(2) and 1.93(2) Å, respectively, were derived clearly showing that the BH$_4^-$ moiety is essentially symmetrically bound in κ^2-fashion similar to Co(II) PCP systems, but in contrast to related Ni(II) PCP complexes.[12] Moreover, the Cr$\cdots$B distance of 2.47(2) Å is also consistent with this binding mode. The Cr-C$_{ipso}$ bond distance is 2.076(2) Å being slightly shorter than in **2**.
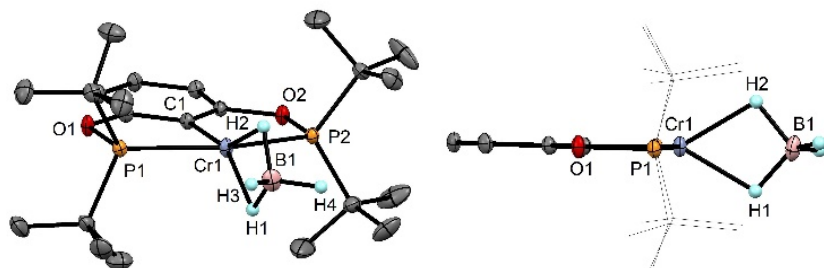
Figure 3. Left: Structural view of [Cr(POCOP-*t*Bu)(κ^2-BH$_4$)] (**3**) showing 50% thermal ellipsoids (most H atoms omitted for clarity). Right: Side view of **3**. Selected bond lengths (Å) and bond angles (°): Cr1-C1 2.076(2), Cr1-P1 2.4464(6), Cr1-P2 2.4515(7), Cr1-H1 1.91(2), Cr1-H2 1.93(2), Cr1-B1 2.47(2), B1-H1 1.25(2), B1-H2 1.31(3), B1-H3 1.12(3), B1-H4 0.96(4), P1-Cr1-P2 154.376(18).

Nitrosylation of complex **3** with nitric oxide at ambient pressure afforded the cationic five coordinate Cr(I) complex [Cr(POCOP-tBu)(NO)(κ^2-BH$_4$)] (**4**) in 88 % isolated yield (Scheme 2).[13] This reaction could be viewed as a formal one electron reduction of the metal center by the NO radical from Cr(II) to Cr(I), if NO is counted as NO$^+$ (*vide infra*). Characterization was accomplished by the solution magnetic (Evans method), IR spectroscopy, EPR, DFT calculations and elemental analysis. In the IR spectrum a strong absorption band assignable to the NO stretching frequency at 1654 cm^{-1} is observed. The terminal and bridging hydrogen-boron stretches ν_{B-Ht} and ν_{B-Hb}, respectively, are observed at 2465, 2427 and 2016 cm^{-1}. As judged by solution magnetic susceptibility measurements (CD$_2$Cl$_2$, Evans method) and an EPR study, this compound is a low-spin complex. The solution effective magnetic moment of 2.0(1) μ_B agrees well with a low-spin d^5 center.
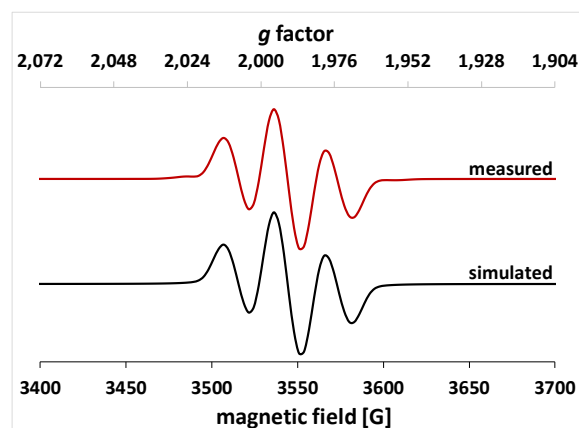

Figure 4. X-band EPR spectrum of [Cr(POCOP-tBu)(NO)(κ^2-BH$_4$)] (**4**) in toluene at 293 K at a microwave frequency of 9.86 GHz. The red line represents a simulation with parameters g_{iso} = 1.9828 and A (^{31}P) = 29.0 G and A (^{14}N) = 5.3 G.

In the X-band EPR spectrum, an isotropic triplet at g_{iso} = 1.9828 with a well-resolved large hyper fine coupling characterized by a 1:2:1 multiplet pattern, originating from the interaction of the unpaired electron with two equivalent ^{31}P (I= 1/2) nuclei to the phosphorous atoms A = 29.0 G (Figure 4). Most reported low-spin {CrNO}^{5} (Cr(I)) systems feature EPR spectra with g values close to 2.0.[14]

The frontier orbitals obtained by DFT for complex **4** are consistent with a low-spin d^5 Cr(I) center possessing a HOMO (single occupied) of largely d_{xy} character (Figure 5). The spin density is essentially centered on the metal and the orbitals (*d*-splitting) are the expected ones for a d^5 low spin pseudo-square pyramid. The bonding and charge distribution are also in agreement with a Cr(I) complex. The metal charge is significantly less positive in **4** (C = 0.04) than in **3** (C = 0.58). All metal-donor bonds are stronger in complex **4** as reflected by the Wiberg indices of the coordinating bonds and on the ligand charges (electron poorer ligands mean stronger donations): WI(Cr-P) = 0.47 (0.41 in **3**), WI(Cr-H) = 0.18 (equatorial) and 0.13 (apical), WI(Cr-N) = 1.64; C(PCP) = 0.50, C(BH$_4$) = -0.45, C(NO) = -0.09. Coordination of the BH$_4^-$ ligand in **4** is asymmetric with a slightly stronger equatorial bond, as shown by the Wiberg indices above. Again, coordination of B-H bonds is reflected on the corresponding bond strength, as stronger B-H → Cr donation result on weaker B–H bonds. Accordingly, the equatorial coordinated B–H has a Wiberg index of 0.71, while the apical one has a value of WI = 0.76. The free B-H bonds have a WI of 0.96.
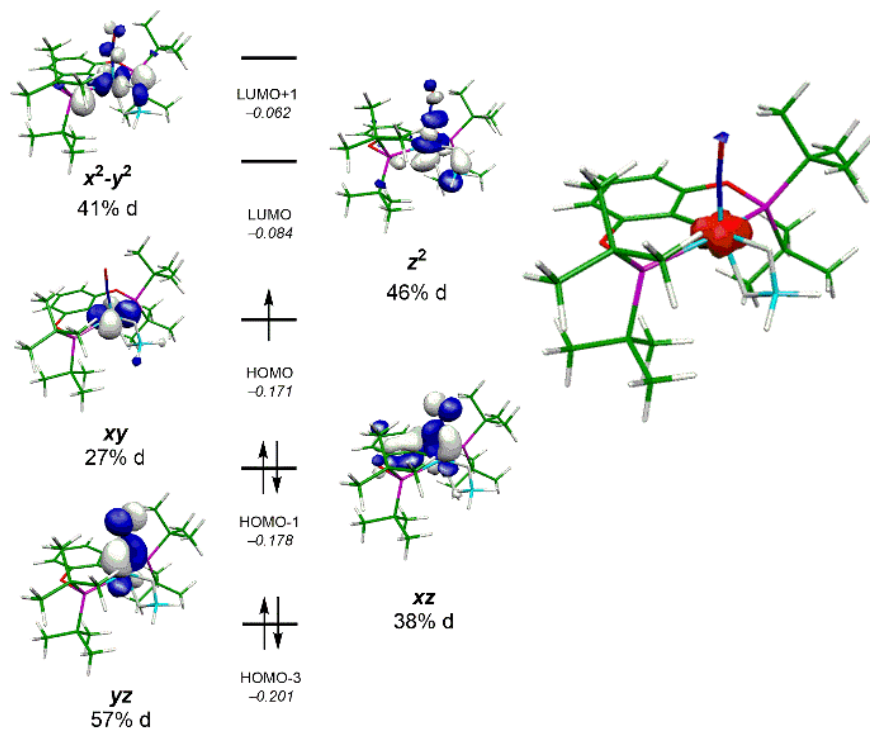
Figure 5. Frontier orbitals (*d*-splitting) and spin density for [Cr(POCOP-*t*Bu)(NO)(κ^2-BH$_4$)] (**4**). Orbital energy values in hartrees (italic)
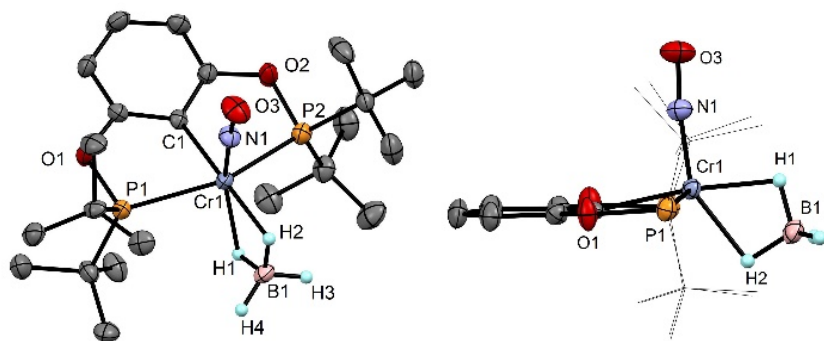
Figure 6. Left: Structural view of [Cr(POCOP-*t*Bu)(NO)(κ^2-BH$_4$)] (**4**) showing 50% thermal ellipsoids (H atoms omitted for clarity). Right: Side view of **4**. Selected bond lengths (Å) and bond angles (°): Cr1-N1 1.658(3), Cr1-C1 2.068(3), Cr1-B1 2.292(4), Cr1-H1 1.90(3), Cr1-H2 1.84(4), Cr1-P1 2.447(1), Cr1-P2 2.461(1), B1-H1 1.13(4), B1-H2 1.11(3), B1-H3 0.98(4), B1-H4 1.05(4), Cr1-N1-O3 173.4(3), P1-Cr1-P2 150.11(4).

A molecular structure of **4** is shown in Figure 6 with selected bond distances and angles given in the caption. The six-coordinate geometry of this complex adopts a distorted octahedral geometry. The Cr-N-O bond angle is 173.4(3)° and is thus nearly linear. This is again consistent with NO being essentially a NO$^+$ cation. The Cr-C$_{ipso}$ bond distance is 2.068(3) Å. The positions of the bridging and terminal hydrides H$_b$ and H$_t$ of the BH$_4^-$ ligand could also be located in the difference Fourier map and refined isotropically. The chromium atom coordinates the BH$_4$-group in a κ^2-fashion but in a slightly asymmetrical fashion with Cr-H$_b$ distances of 1.90(3) and 1.84(4) Å. The Cr-B distance is 2.292(4) Å.

Scheme 3. Synthesis of Complexes 4 and 5
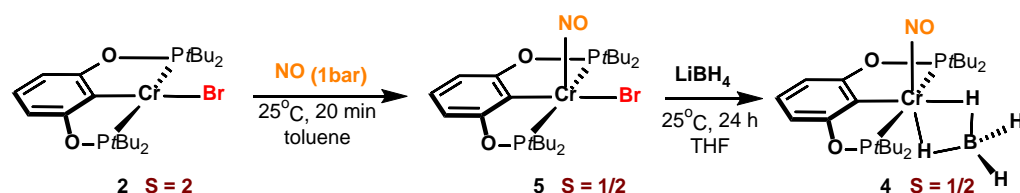
Complex **4** could be also prepared *via* an alternative route. Exposure of a toluene solution of **2** to NO (1 bar) at room temperature affords [Cr(POCOP-*t*Bu)(NO)(Br)] (**5**) in 95% isolated yield (Scheme 3). This reaction again can be viewed as a formal one electron reduction of the metal center by the NO radical from Cr(II) to Cr(I). EPR studies (see SI) and solution magnetic susceptibility measurements (CD$_2$Cl$_2$, Evans method) clearly show that this compound is a low-spin complex. The solution effective magnetic moment of 1.8(4) μ_B is in agreement with a low-spin d^5 center (one unpaired electron). Complex **5** exhibits a strong band at 1654 cm^{-1} in the IR spectrum assignable to the NO frequency. In the X-band EPR spectrum, recorded in CH$_2$Cl$_2$ at 298 K, this compound displays an isotropic multiplet at g$_{iso}$ = 1.9963 with a well-resolved hyper fine coupling to the nitrogen and phosphorous atoms (A$_N$ = 5.5 and A$_P$ = 26.9 G) and again is consistent with low-spin Cr(I) (S = ½).

A structural view of **5** is shown in Figure 7 with selected bond distances and angles provided in the caption. The five-coordinate geometry of this complex is best described as a distorted square-pyramid with NO in the apical and the PCP and Br ligands in the basal position. The Cr-N-O bond angle is 177.3(3)° and the Cr-N-O moiety can be thus considered as nearly linear. This is consistent with NO being essentially a NO$^+$ cation. The Cr-C$_{ipso}$ bond distance is 2.056(2) Å.
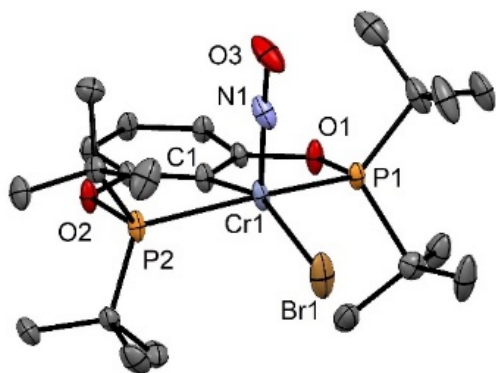
Figure 7. Structural view of [Cr(POCOP-*t*Bu)(NO)(Br)] (**5**) showing 50% thermal ellipsoids (H atoms omitted for clarity). Selected bond lengths (Å) and bond angles (°): Cr1-C1 2.056(2), Cr1-P1 2.416(3), Cr1-P2 2.430(2), Cr1-Br1 2.414(2), Cr1-N1 1.664(4), P1-Cr1-P2 152.54(7), C1-Cr1-Br1 150.98(8), Cr1-N1-O3 177.3(3).

When **5** is reacted with 2 equiv of LiBH$_4$ in THF for 24 h the borohydride complex [Cr(POCOP-*t*Bu)(NO)(κ^2-BH$_4$)] (**4**) was obtained in 91% isolated yield (Scheme 3).

The mechanism of NO addition to **3** was investigated by means of DFT calculations. A free energy profile is depicted in Figure 8. The reaction proceeds along the spin quintet potential energy surface, starting with **B** the pair of reactants of **3** and NO (NO being a doublet) producing complex **C** *via* transition state **TS$_{BC}$**. In this transition state the new Cr-N bond is only incipient with a distance of 3.01 Å which is still far away from the coordination distance of 2.21 Å in **C**. The energy barrier is 19 kcal/mol (from the separated reactants, **A**). The reaction then proceeds from **C** to **D** with a change in spin state from quintet (S = 5/2) to doublet (S = 1/2). The minimum energy crossing point **CP** between the potential energy surfaces of the two spin states is easily accessible lying merely 1 kcal/mol above **C** and the formation of **D** is exergonic by -16 kcal/mol (with respect to **A**). In agreement with experimental data, [Cr(POCOP-*t*Bu)(NO)(κ^2-BH$_4$)] (**4**) adopts a doublet rather than a quintet ground state.
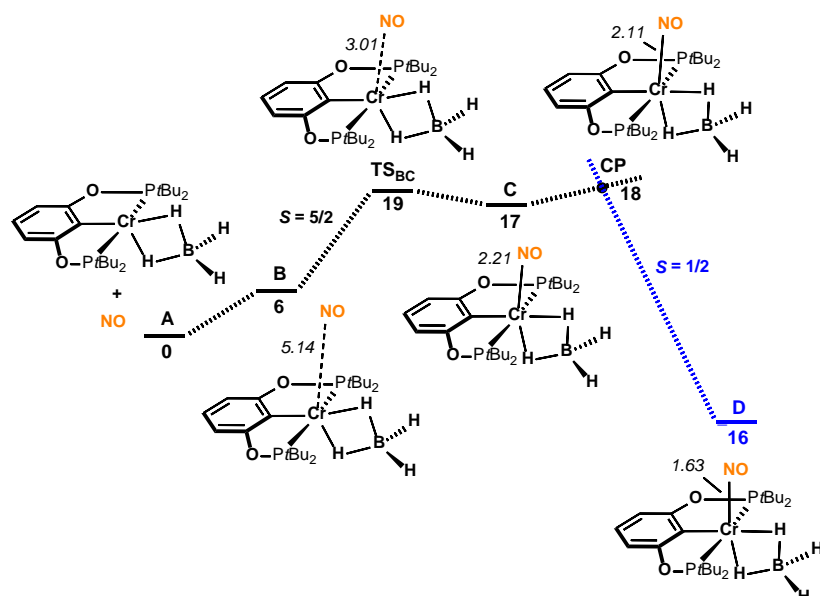
Figure 8. Free Energy Profile Calculated for the Nitroslyation of **3**. Free Energies (kcal/mol) are Referred to **A** (**3** + NO)). Bond Distances (Å) are in Italic.

Treatment of **2** with 1 equiv of Li(CH₂SiMe₃ in toluene for 4 h afforded the alkyl complex [Cr(POCOP-*t*Bu)(CH₂SiMe₃] (**6**) in 57 % isolated yield as red solid (Scheme 4). Solution magnetic susceptibility measurements (C₆D₆, Evans method) clearly show that this complex is a d⁴-high-spin complex with an effective magnetic moment of 4.8(2) μ$_B$. A structural view of **6** is shown in Figure 9 with selected bond distances and angles reported in the caption. The coordination geometry around the chromium center is best described by a slightly distorted square-planar arrangement. The C1-Cr1-C2 angle deviates from linearity being 168.91(8)°. The P(1)-Cr1-P2 angle is 152.15(2)°. The Cr-C$_{ipso}$ and the Cr-C$_{alkyl}$ bond distances are 2.123(2) 2.145(2) Å, respectively.

Scheme 4 Synthesis of Complex 6
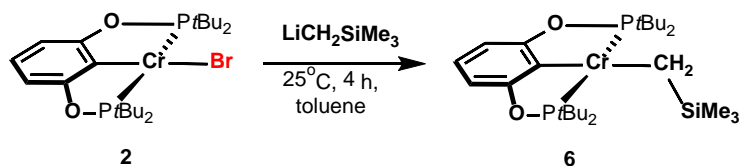
Since a Cr(II) alkyl complex was recently shown to be catalytically active for the hydrosilylation of ketones,[15] we begun to investigate the potential the Cr(II) PCP alkyl complex **6** as catalyst for this transformation. Complex **6** (0.5 mol % based on ketones) was reacted with both aromatic and aliphatic ketones and (MeO)₃SiH (1.2 equiv) in toluene (3 mL) at 25 °C. The results are summarized in Table 1. After workup with K₂CO₃/MeOH, all alcohols were isolated in yields up to 96% and were characterized by ¹H and ¹³C{¹H} NMR spectroscopy. In general, isolated yields are reported.
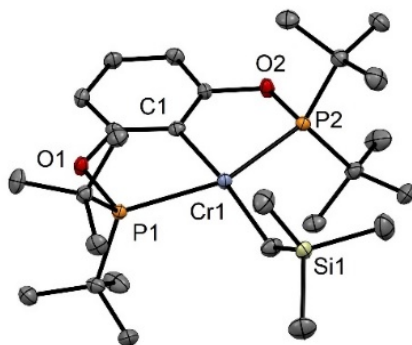
Figure 9. Structural view of [Cr(POCOP-*t*Bu)(CH$_2$SiMe$_3$] (**6**) showing 50% thermal ellipsoids (H atoms omitted for clarity). Selected bond lengths (Å) and bond angles Cr1-C1 2.123(2), Cr1-C7 2.145(2), Cr1-P1 2.4722(7), Cr1-P2 2.4719(7), C1-Cr1-C7 168.91(8), P1-Cr1-P2 152.15(2).

Table 1. Hydrosilylation of Ketones with (MeO)$_3$SiH Catalyzed by [Cr(POCOP-*t*Bu)(CH$_2$SiMe$_3$] (**6**)[a,b]
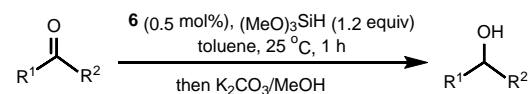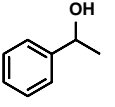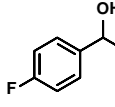
product	product
79%	96%
70%	80%
32%	88%
77%	87%
96%	94%
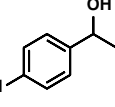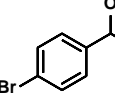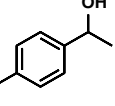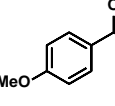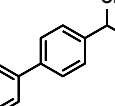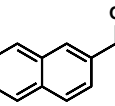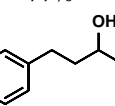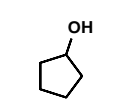
[a] Reaction conditions: 1.12 mmol ketone, 1.34 mmol (MeO)$_3$SiH, 0.5 mol % catalyst, 3 mL toluene, 1 h, 25°C. [b] Isolated yields.

CONCLUSION

The preparation of the Cr(II) PCP complex [Cr(POCOP-*t*Bu)Br] (**2**) via a solvothermal reaction of [Cr(CO)$_6$] with the ligand precursor PO(C-Br)OP-*t*Bu (**1**) is described. Treatment of **2** with LiBH$_4$ in THF for 24 h afforded the borohydride complex [Cr(POCOP-*t*Bu)(κ^2-BH$_4$)] (**3**). Exposure of a toluene solution of **3** to NO gas (1 bar) at room temperature gave the Cr(I) complex [Cr(POCOP-*t*Bu)(NO)(κ^2-BH$_4$)] (**4**). Alternatively, **4** was also obtained by reacting [Cr(POCOP-*t*Bu)(NO)(Br)] (**5**) with Li[HBEt$_3$]. Based on magnetic and EPR measurements as well as DFT calculations, compounds **4** and **5** were found to adopt a low-spin d^5 configuration and feature a nearly linear bound NO ligand suggesting Cr^{I}NO$^+$ rather than Cr^{II}NO$^\bullet$ character. Reacting **2** with 1 equiv of LiCH$_2$SiMe$_3$ in toluene afforded the square planar alkyl complex [Cr(POCOP-*t*Bu)(CH$_2$SiMe$_3$] (**6**) in 57% yield. This compound is catalytically active for the hydrosilylation of ketones with (MeO)$_3$SiH at room temperature with a catalyst loading of as low as 0.5 mol%. X-ray structures of all complexes are presented.

EXPERIMENTAL SECTION

General Information. All reactions were performed under an inert atmosphere of argon by using Schlenk techniques or in a MBraun inert-gas glovebox. The solvents were purified according to standard procedures.[16] The deuterated solvents were purchased from Aldrich and dried over 3 Å molecular sieves. All starting materials are known compounds and were used as obtained from commercial resources. ^{1}H and ^{13}C{^{1}H}, and ^{31}P{^{1}H} NMR spectra were recorded on Bruker AVANCE-250, AVANCE-400, and AVANCE-600 spectrometers. ^{1}H and ^{13}C{^{1}H} NMR spectra were referenced internally to residual protio-

solvent, and solvent resonances, respectively, and are reported relative to tetramethylsilane ($\delta = 0$ ppm). ^{31}P{^{1}H} NMR spectra were referenced externally to H$_3$PO$_4$ (85%) ($\delta = 0$ ppm).

High resolution-accurate mass data mass spectra were recorded on a hybrid Maxis Qq-aoTOF mass spectrometer (Bruker Daltonics, Bremen, Germany) fitted with an ESI-source. Measured accurate mass data of the [M]$^+$ ions for confirming calculated elemental compositions were typically within ±5 ppm accuracy. The mass calibration was done with a commercial mixture of perfluorinated trialkyl-triazines (ES Tuning Mix, Agilent Technologies, Santa Clara, CA, USA).

CW-EPR spectroscopic measurements were performed on an X-band Bruker Elexsys-II E500 EPR spectrometer (Bruker Biospin GmbH, Rheinstetten, Germany) in solution at 293 K. A high sensitivity cavity (SHQE1119) was used for measurements setting the microwave frequency to 9.86 GHz, the modulation frequency to 100 kHz, the center field to 6000 G, the sweep width to 12000 G, the sweep time to 30.0 s, the modulation amplitude to 6 G, the microwave power to 15.9 mW, the conversion time to 7.33 ms and the resolution to 4096 points. The spectra were analyzed using the Bruker Xepr software.

PO(C-Br)OP-*t*Bu (1). To a solution of 2-bromorecinol (0.48 g, 2.5 mmol) in THF (20 mL) NEt$_3$ (0.55 g, 5.4 mmol) and *t*Bu$_2$PCl (1.0 mL, d = 0.95 g/mL, 96%, 5.2 mmol) was added and the reaction mixture was stirred for 6 days at 80 °C. After cooling to room temperature, the solvent was removed under reduced pressure and *n*-pentane (15 mL) was added. Then the reaction mixture was filtered over a small pad of silica gel and washed two times with toluene (10 mL). All volatiles were removed at reduced pressure and the white solid was dissolved in toluene and filtered again over a pad of silica gel to remove the remaining solid impurities. All volatiles were removed under reduced pressure and the white solid was dried under vacuum. Yield: 0.8 g (66%). ^{1}H NMR (δ, 400 MHz, CD$_2$Cl$_2$, 20 °C): 7.05 (m, 3H, C$_{ar}$*H*), 1.19 (d, *J* = 11.9 Hz, 36H, *t*Bu). ^{13}C{^{1}H} NMR (δ, 400MHz, CD$_2$Cl$_2$, 20 °C): 157.8 (d, *J* = 10.1 Hz, *C*$_{ar}$), 127.6 (s, *C*$_{ar}$H), 110.5 (d, *J* = 22.2 Hz, *C*$_{ar}$H), 105.2 (s, *C*$_{ar}$), 36.2 (d, *J* = 26.1 Hz, P-*C*), 27.5 (d, *J* = 15.6 Hz, *C*H$_3$). ^{31}P{^{1}H} NMR (δ, 400 MHz, CD$_2$Cl$_2$, 20 °C): 156.3. HR-MS (ESI$^+$, CH$_3$CN/MeOH + 1% H$_2$O): m/z calcd for C$_{22}$H$_{40}$BrO$_2$P$_2$ [M+H]$^+$ 477.1687, found 477.1672.

[Cr(POCOP-*t*Bu)(Br)] (2). A suspension of Cr(CO)$_6$ (47 mg, 0.21 mmol) and **1** (100 mg, 0.21 mmol) in toluene (3 mL) was placed in a 20 mL sealed glass tube and stirred for 3 h at 180 °C. The pure product could be obtained directly from the reaction mixture as red crystals which were washed with *n*-pentane (2 mL) and dried under vacuum. Yield: 90 mg (76%). Anal. Calcd for C$_{22}$H$_{39}$BrCrO$_2$P$_2$ (529.40): C, 49.91; H, 7.43. Found: C, 49.46; H, 7.28. μ_{eff} = 4.8(4) μ_B (CD$_2$Cl$_2$, Evans method).

[Cr(POCOP-*t*Bu)(κ^2-BH$_4$)] (3). To a solution of **2** (25 mg, 0.047 mmol) in THF (4 mL) LiBH$_4$ (2 mg, 0.09 mmol) was added and the mixture was stirred at for 24 h at room temperature. All volatiles were removed under reduced pressure and the residue was dissolved in CH$_2$Cl$_2$ (2 mL) and filtered over a pad of basic Al$_2$O$_3$. Volatiles were again removed under reduced pressure and the remaining orange solid was washed twice with n-pentane (3 mL) and dried under vacuum. Yield: 19 mg (86%). Anal. Calcd for C$_{22}$H$_{43}$BCrO$_2$P$_2$ (464.34): C, 56.91; H, 9.33. Found: C, 56.53; H, 9.11. μ_{eff} = 4.9(4) μ_B (CD$_2$Cl$_2$, Evans method). IR (ATR, cm^{-1}): 2407 (ν_{BH}), 2068 (ν_{BH}).

[Cr(POCOP-*t*Bu)(NO)(κ^2-BH$_4$)] (4). Method A: A solution of **3** (20 mg, 0.036 mmol) in THF (4 mL) was reacted with LiBH$_4$ (2 mg, 0.09 mmol) at room temperature for 24 h, whereupon the color of the solution changed from black to intensive red. All volatiles were then removed under reduced pressure and the solid residue was dissolved in CH$_2$Cl$_2$ (2 mL) and filtered over a pad of basic Al$_2$O$_3$. Volatiles were removed under reduced pressure and the remaining solid was dried under vacuum. Yield: 16 mg (91%). **Method B:** Nitric oxide was bubbled into a solution of **5** (20 mg, 0.043 mmol) in toluene (3 mL) for ca. 0.5 min and the mixture was stirred for 15 min. All volatiles were removed under reduced pressure yielding 19 mg (88%) of **4** as a brown solid. Anal. Calcd for C$_{22}$H$_{43}$BCrNO$_3$P$_2$ (494.34): C, 53.45; H, 8.77; N, 2.83. Found: C, 53.65; H, 8.43; N, 3.00. μ_{eff} = 2.0(1) μ_B (CD$_2$Cl$_2$, Evans method). IR (ATR, cm^{-1}): 2465 (ν_{BH}), 2427 (ν_{BH}), 2016 (ν_{BH}), 1654 (ν_{NO}).

[Cr(POCOP-*t*Bu)(NO)(Br)] (5). Nitric oxide was bubbled into a solution of **2** (25 mg, 0.047) in toluene (3 mL) for ca. 0.5 min and the mixture was stirred for 20 min, whereupon the reaction mixture turned from red to black. After removal of all volatiles under reduced pressure, the remaining solid was washed with *n*-pentane (6 mL) and dried under vacuum. Yield: 25 mg (95%). Anal. Calcd for C$_{22}$H$_{39}$BrCrNO$_3$P$_2$ (559.41): C, 47.24; H, 7.03; N, 2.50. Found: C, 47.49; H, 6.92; N, 2.68. μ_{eff} = 1.8(4) μ_B (CD$_2$Cl$_2$, Evans method). IR (ATR, cm^{-1}): 1654 (ν_{NO}).

[Cr(POCOP-*t*Bu)(CH$_2$Si(CH$_3$)$_3$] (6). To a solution of **2** (115 mg, 0.217 mmol) in toluene (6 mL) Li(CH$_2$Si Si(CH$_3$)$_3$ (0.23 mL, 1 M, 0.23 mmol) was added and stirred at room temperature for 4 h. All volatiles were then removed under reduced pressure and the crude product was dried for 20 min under vacuum. The residue was re-dissolved in *n*-pentane (1 mL) and filtered over a syringe filter (PTFE, 0.2 µm). The saturated solution was placed into the freezer at -20 °C for 24 h resulting in the formation of red crystals. Yield: 67 mg (57%). Anal. Calcd for C$_{26}$H$_{50}$CrO$_2$P$_2$Si (536.71): C, 58.18; H, 7.03. Found: C, 58.27; H, 7.16. μ_{eff} = 4.8(4) μ_B (C$_6$D$_6$, Evans method).

Hydrosilylation of Ketones. To a solution of **6** (3 mg, 5.6 µmol, 0.5 mol%) in toluene (3 mL) substrate (1.12 mmol, 1 equiv) and (MeO)$_3$SiH (0.17 ml, 1.34 mmol, 1.2 equiv) was added and the mixture was stirred for 1 h at 25 ºC. A saturated K$_2$CO$_3$ solution (5 mL) in MeOH was then added. After 2 h of stirring, solvent was removed under vacuum and the crude product was dissolved in CH$_2$Cl$_2$ (5 mL). Silica gel (1.0 g) was added and the mixture was stirred for 1 h and then filtered

through a glass frit. After removal of all volatiles the resulting alcohols were characterized by ^{1}H and ^{13}C{^{1}H} NMR spectroscopy.

X-ray Structure Determination. X-ray diffraction data of **2**–**6** (CCDC 1945159–1935161, 1956770, 1956771) were collected at $T = 100$ K in a dry stream of nitrogen on a Bruker Kappa APEX II diffractometer system using graphite-monochromatized Mo-$K\alpha$ radiation ($\lambda = 0.71073$ Å) and fine sliced φ- and ω-scans. For **4**, reflections of two twin domains were identified using the RLATT tool. Data were reduced to intensity values with SAINT and an absorption correction was applied with the multi-scan approach implemented in SADABS or TWINABS.[17]The structures were solved by the dual-space approach implemented in SHELXT[18] and refined against F^2 with Jana2006[19] (**2**, **3**, **5**) or SHELXL[20] (**4**, **6**). Non-hydrogen atoms were refined anisotropically. The H atoms connected to C atoms were placed in calculated positions and thereafter refined as riding on the parent atoms. The hydride-Hs were located from difference Fourier maps and refined freely. **3** co-crystallized with **2** in a ~95:5 ratio. The triclinic **2** and **3** crystallize in polytypic structures, which causes twinning (**3**) and appearance of ghost atoms (**2**) corresponding to alternative stacking possibilities. To simplify structural descriptions and refinement, the structures are described based on non-reduced settings, where the layers lie in the (001) plane. The Cr, Br and P atoms of the second orientation of **2** (realized for ca. 4% of the layers) were refined freely using anisotropic displacement parameters. The lighter atoms were restrained to fixed coordinates and ADPs related to the major orientation by a $2_{[010]}$ operation. Details of the polytypism will be detailed in an upcoming publication. The **4** complex was disordered over two orientations in a 87.74:12.14 ratio. The ADPs of some atoms of the minor orientation were restrained to be identical to the corresponding atoms in the major orientation.

Computational Details. The computational results presented have been achieved in part using the Vienna Scientific Cluster (VSC). Calculations were performed using the GAUSSIAN 09 software package[21] and the OPBE functional without symmetry constraints. This functional combines Handy's OPTX modification of Becke's exchange functional[22] with the gradient corrected correlation functional of Perdew, Burke, and Ernzerhof,[23] and it was shown to be accurate in the calculation of spin state energy splitting for first transition row species.[24] The optimized geometries were obtained with the Stuttgart/Dresden ECP (SDD) basis set[25] to describe the electrons of Cr and a standard 6-31G** basis set[26] for the other atoms. Transition state optimization was performed with the Synchronous Transit-Guided Quasi-Newton Method (STQN) developed by Schlegel *et al*,[27] following an extensive search of the Potential Energy Surface. Frequency calculations were performed to confirm the nature of the stationary points, yielding one imaginary frequency for the transition state and none for the minima. The transition state was further confirmed by following its vibrational mode downhill on both sides, and obtaining the minima presented on the energy profiles. The electronic energies were converted to free energy at 298.15 K and 1 atm by using zero-point energy and thermal energy corrections based on structural and vibration frequency data calculated at the same level. A Natural Population Analysis (NPA)[28] and the resulting Wiberg indices[7] were used to study the electronic structure and bonding of the optimized species. The NPA analysis was performed with the *NBO 5.0* program,[29] Orbital representations were obtained with Molekel.[30] Complex **4** orbitals (Figure 5, left side) result from a single point restricted open-shell calculation.

The Minimum Energy Crossing Point (**CP**) between the spin doublet ($S = 1/2$) and the spin sextet ($S = 5/2$) Potential Energy Surfaces (PES) was determined using a code developed by Harvey *et al*.[31] This code consists of a set of shell scripts and Fortran programs that uses the Gaussian results of energies and gradients of both spin states to produce an effective gradient pointing towards the **CP**. This is not a stationary point and, hence, a standard frequency analysis is not applicable. Therefore, the free energy value of the crossing point (**CP**) was obtained through frequency calculations projected for vibrations perpendicular to the reaction path.[32] The value presented is the mean of the values obtained for both PES.

REFERENCES

(1) Coining of the name "pincer": van Koten, Tuning the reactivity of metals held in a rigid ligand environment G. *Pure App. Chem.* **1989**, *61*, 1681-1694.

(2) For reviews on pincer complexes, see: (a) Gossage, R. A.; van de Kuil, L. A.; van Koten, G. Diaminoarylnickel(II) "pincer" complexes: mechanistic consideration in the Kharasch addition reaction, controlled polymerization, and dendrimeric transition metal catalysis *Acc. Chem. Res.* **1998**, *31*, 423-431. (b) Albrecht, M.; van Koten, G. Platinum group organometallics based on "Pincer" complexes: sensors, switches, and catalysts in memory of Prof. Dr. Luigi M. Venanzi and his pioneering work in organometallic chemistry, particularly in PCP pincer chemistry *Angew. Chem., Int. Ed.* **2001**, *40*, 3750-3781. (c) van der Boom, M. E.; Milstein, D. Cyclometalated phosphine-based pincer complexes: mechanistic insight in catalysis, coordination, and bond activation *Chem. Rev.* **2003**, 103, 1759-1792. (d) Singleton, J. T. The uses of pincer complexes in

organic synthesis *Tetrahedron* **2003**, *59*, 1837-1857. (e) Liang, L. C. Metal complexes of chelating diarylamido phosphine ligands *Coord. Chem. Rev.* **2006**, 250, 1152-1177. (f) The Chemistry of Pincer Compounds; Morales-Morales, D.; Jensen, C. M.; Eds.; Elsevier: Amsterdam, **2007**. (g) Nishiyama, H. Synthesis and use of bisoxazolinyl-phenyl pincers *Chem. Soc. Rev.* **2007**, 36, 1133-1141. (h) Benito-Garagorri, D.; Kirchner, K. Modularly Designed Transition Metal PNP and PCP Pincer Complexes Based on Aminophosphines: Synthesis and Catalytic Applications *Acc. Chem. Res.* **2008**, *41*, 201-213. (i) Choi, J.; MacArthur, A. H. R.; Brookhart, M.; Goldman, A. S. Dehydrogenation and Related Reactions Catalyzed by Iridium Pincer Complexes *Chem. Rev.* **2011**, 111, 1761-1779. (j) Selander, N.; Szabo, K. J. Catalysis by Palladium Pincer Complexes *J. Chem. Rev.* **2011**, 111, 2048-2076. (k) Bhattacharya, P.; Guan, H. Synthesis and Catalytic Applications of Iron Pincer Complexes *Comment Inorg. Chem.* **2011**, 32, 88-112. (l) Schneider, S.; Meiners, J.; Askevold, B. Cooperative Aliphatic PNP Amido Pincer Ligands - Versatile Building Blocks for Coordination Chemistry and Catalysis *Eur. J. Inorg. Chem.* **2012**, 412-429. (m) van Koten, G.; Milstein, D. Eds.; Organometallic Pincer Chemistry; Springer: Berlin, **2013**; *Top. Organomet. Chem.* Vol. 40. (n) Szabo, K. J.; Wendt, O. F., Pincer and Pincer-Type Complexes: Applications in Organic Synthesis and Catalysis, Wiley-VCH, Germany, **2014**. (o) Asay, M.; Morales-Morales, D. Non-symmetric pincer ligands: complexes and applications in catalysis *Dalton Trans.* **2015**, *44*, 17432-17447. (p) Murugesan, S.; Kirchner, K. Non-precious metal complexes with an anionic PCP pincer architecture *Dalton Trans.* **2016**, *45*, 4163-439.

(3) For recent reviews on C-H activation and functionalization, see, (a) Jia, C.; Kitamura, T.; Fujiwara, Y. Catalytic Functionalization of Arenes and Alkanes via C−H Bond Activation *Acc. Chem. Res.* **2001,** *34*, 633-639. (b) Ritleng, V.; Sirlin, C.; Pfeffer, M. Ru-, Rh-, and Pd-Catalyzed C−C Bond Formation Involving C−H Activation and Addition on Unsaturated Substrates: Reactions and Mechanistic Aspects *Chem. Rev.*, **2002**, *102*, 1731–1770. (c) Colby, D. A.; Bergman, R. G.; Ellman, J. A. Rhodium-Catalyzed C−C Bond Formation via Heteroatom-Directed C−H Bond Activation *Chem. Rev.*, **2010**, *110*, 624-655. (d) Arockiam, P. B.; Bruneau, C.; Dixneuf, P. H. Ruthenium(II)-Catalyzed C–H Bond Activation and Functionalization *Chem. Rev.*, **2012**, *112*, 5879-5918. (e) Lewis, J. C.; Bergman, R. G.; Ellman, J. A. Direct Functionalization of Nitrogen Heterocycles via Rh-Catalyzed C−H Bond Activation *Acc. Chem. Res.*, **2008**, *41*, 1013-1025. (f) Gaillard, S.; Cazin, C. S. J.; Nolan S. P. N-Heterocyclic Carbene Gold(I) and Copper(I) Complexes in C–H Bond Activation *Acc. Chem. Res.*, **2012**, *45*, 778–787. (g) Li, B.; Dixneuf, P. H. sp^2 C–H bond activation in water and catalytic cross-coupling reactions *Chem. Soc. Rev.* **2013**, *42*, 5744-5767. (h) Wencel-Delord, J.; Dröge, T.; Liu, F.; Glorius, F. Towards mild metal-catalyzed C–H bond activation *Chem. Soc. Rev.* **2011**, *40*, 4740-4761.

(4) For related Cr(II) pincer complexes see: (a) Schiwek, C. H.; Vasilenko, V.; Wadepohl, H.; Gade, L. H. The open d-shell enforces the active space in 3d metal catalysis: highly enantioselective chromium(II) pincer catalysed hydrosilylation of ketones *Chem. Commun.* **2018**, *54*, 9139-9142. (b) Simler, T.; P. Braunstein, P.; Danopoulos, A. A. Chromium(II) Pincer Complexes with Dearomatized PNP and PNC Ligands: A Comparative Study of Their Catalytic Ethylene Oligomerization Activity *Organometallics* **2016**, *35*, 4044–4049. (c) McGowan, K. P.; Abboud, K. A.; Veige, A. S. Trianionic NCN^{3-} Pincer Complexes of Chromium in Four Oxidation States (Cr^{II}, Cr^{III}, Cr^{IV}, Cr^{V}): Determination of the Active Catalyst in Selective 1-Alkene to 2-Alkene Isomerization *Organometallics* **2011**, *30*, 4949–4957.

(5) Sutton, A. D.; Ngyuen, T.; Fettinger, J. C.; Olmstead, M. M.; Long, G. J.; Power, P. P. Synthesis and Characterization of Low-Coordinate Divalent Aryl Transition-Metal Halide Analogues of Grignard Reagents: Precursors for Reduction to Metal−Metal-Bonded Complexes *Inorg. Chem.* **2007**, *46*, 4809-4814.

(6) The complex geometry can also be viewed as pseudo-square planar with the two B–H bonds occupying one coordination position.

(7) (a) Wiberg, K. B. Application of the pople-santry-segal CNDO method to the cyclopropylcarbinyl and cyclobutyl cation and to bicyclobutane *Tetrahedron* **1968**, *24*, 1083-1096. (b) Wiberg indices are electronic parameters related with the electron density in between two atoms, which scale as bond strength indicators. They can be obtained from a Natural Population Analysis.

(8) Koola, J. D.; Brintzinger, H. H. Synthesis and reactions of η-cyclopentadienylhydridotris(trimethyl phosphite)chromium(II) *J. Chem. Soc. Chem. Commun.* **1976**, 388-389.

(9) Nöth, H.; Seitz, M. Preparation and characterization of chromium(II) tetrahydroborate–tetrahydrofuran *J. Chem. Soc. Chem. Commun.* **1976**, 1004.

(10) Barron, A. R.; Scott, GJ. E.; Wilkinson, G.; M. Motevalli, M.; Hursthouse, M. B. Tertiary phosphine borohydrido complexes of chromium, tungsten and rhenium: crystal structure of *trans*-hydrido(η2-tetrahydroborato)bis[1,2-bis(dimethylphosphino) ethane]chromium(II) *Polyhedron* **1986**, *5*, 1833-1837.

(11) Dionne, M.; Hao, S.; Gambarotta, S. Preparation and characterization of a new series of Cr(ll) hydroborates *Can. J. Chem.* **1995**, *73*, 1126-1134.

(12) Murugesan, S.; Stöger, B.; Veiros, L. F.; Kirchner, K. Synthesis, Structure, and Reactivity of Co(II) and Ni(II) PCP Pincer Borohydride Complexes *Organometallics*, **2015***, 34*, 1364-1372.

(13) Døssing, A. Recent advancs in the chemistry of nitrosyl complexes of chromium *Rev. Inorg. Chem.* **2013**, *33*, 129-137.

(14) (a) van der Eide, E. F.; Helm, M. L.; Walter, E. D.; Bullock, R. M. Structural and Spectroscopic Characterization of 17- and 18-ElectronPiano-Stool Complexes of Chromium. Thermochemical Analyses of Weak Cr−H Bonds *Inorg. Chem.* **2013**, *52*, 1591-1603. (b) Rieger, P. H. Electron paramagnetic resonance studies of low-spin d^5 transition metal complexes *Coord. Chem. Rev.* **1994**, *135/136*, 203−286. (c) Carruthers, L. M.; Closken, C. L.; Link, K. L.; Mahapatro, S. N.; Bikram, M.; Du, J.-L.; Eaton, S. S.; Eaton, G. R. Electron Spin Relaxation in Chromium-Nitrosyl Complexes *Inorg. Chem.* **1999**, *38*, 3529-3534. (d) Cummings, D. A.; McMaster, J.; Rieger, A. L.; Rieger, P. H. EPR Spectroscopic and Theoretical Study of Chromium(I) Carbonyl Phosphine and Phosphonite Complexes *Organometallics* **1997**, *16*, 4362-4368. (e) Luckham, S. L. J.; Folli, A.; Platts, J. A.; Emma Richards, E.; Murphy, D. M. Unravelling the Photochemical Transformations of Chromium(I) 1,3-Bis(diphenylphosphino), $[Cr(CO)_4(dppp)]^+$, by EPR Spectroscopy *Organometallics* **2019**, *38*, 2523−2529. (f) Carter, E.; Cavell, K. J.; Gabrielli, W. F.; Hanton, M. J.; Hallett,A. J.; McDyre, L. E.; Platts, J. A.; Smith, D. M.; Murphy, D. M.Formation of $[Cr(CO)x(Ph_2PN(iPr)PPh_2)]^+$ Structural Isomers by Reaction of Triethylaluminum with a Chromium N,N-Bis-(diarylphosphino)amine Complex $[Cr(CO)_4(Ph_2PN(iPr)(PPh_2)]^+$: An EPR and DFT Investigation *Organometallics* **2013**, *32*, 1924−1931.

(15) Schiwek, C. H.; Vasilenko, V.; Wadepohl, H.; Gade, L. H. The open d-shell enforces the active space in 3d metal catalysis: highly enantioselective chromium(II) pincer catalyzed hydrosilylation of ketones *Chem. Commun.* **2018**, *54*, 9139-9142.

(16) Perrin, D. D.; Armarego, W. L. F. *Purification of Laboratory Chemicals*, 3rd ed.; Pergamon: New York, **1988**.

(17) Bruker computer programs: RLATT, APEX2, SAINT, SADABS, and TWINABS (Bruker AXS Inc., Madison, WI, **2019**).

(18) Sheldrick, G. M. Crystal structure refinement with SHELXL *Acta Crystallogr.* **2015**, *A71*, 3–8.

(19) Petříček, V.; Dušek, V. M.; Palatinus, L. Crystallographic Computing System JANA2006: General features *Z. Kristallogr.* **2014**, *229*, 345–348.

(20) Sheldrick, G. M. Crystal structure refinement with SHELXL *Acta Crystallogr.* **2015**, *C71*, 3–8.

(21) Gaussian 09, Revision A.02, Frisch, M. J.; Trucks, G. W.; Schlegel, H. B.; Scuseria, G. E.; Robb, M. A.; Cheeseman, J. R.; Scalmani, G.; Barone, V.; Mennucci, B.; Petersson, G. A.; Nakatsuji, H.; Caricato, M.; Li, X.; Hratchian, H. P.; Izmaylov, A. F.; Bloino, J.; Zheng, G.; Sonnenberg, J. L.; Hada, M.; Ehara, M.; Toyota, K.; Fukuda, R.; Hasegawa, J.; Ishida, M.; Nakajima, T.; Honda, Y.; Kitao, O.; Nakai, H.; Vreven, T.; Montgomery, Jr., J. A.; Peralta, J. E.; Ogliaro, F.; Bearpark, M.; Heyd, J. J.; Brothers, E.; Kudin, K. N.; Staroverov, V. N.; Kobayashi, R.; Normand, J.; Raghavachari, K.; Rendell, A.; Burant, J. C.; Iyengar, S. S.; Tomasi, J.; Cossi, M.; Rega, N.; Millam, J. M.; Klene, M.; Knox, J. E.; Cross, J. B.; Bakken, V.; Adamo, C.; Jaramillo, J.; Gomperts, R.; Stratmann, R. E.; Yazyev, O.; Austin, A. J.; Cammi, R.; Pomelli, C.; Ochterski, J. W.; Martin, R. L.; Morokuma, K.; Zakrzewski, V. G.; Voth, G. A.; Salvador, P.; Dannenberg, J. J.; Dapprich, S.; Daniels, A. D.; Farkas, Ö.; Foresman, J. B.; Ortiz, J. V.; Cioslowski, J.; Fox, D. J. Gaussian, Inc., Wallingford CT, **2009**.

(22) (a) Handy, N. C.; Cohen, A. Left-right correlation energy *J. Mol. Phys.* **2001**, *99*, 403-412; (b) Hoe, H.-M.; Cohen, A.; Handy, N. C. Assessment of a new local exchange functional OPTX *Chem. Phys. Lett.* **2001**, *341*, 319-328.

(23) (a) Perdew, J. P.; Burke, K.; Ernzerhof, M. Generalized Gradient Approximation Made Simple *Phys. Rev. Lett.* **1996**, *77*, 3865-3868; (b) Perdew, J. P.; Burke, K.; Ernzerhof, M. Generalized Gradient Approximation Made Simple *Phys. Rev. Lett.* **1997**, *78*, 1396-1396.

(24) (a) Swart, M. Accurate Spin-State Energies for Iron Complexes *J. Chem. Theory Comput.* **2008**, *4*, 2057-2066; (b) Conradie, J.; Ghosh, A. Electronic Structure of Trigonal-Planar Transition-Metal-Imido Complexes: Spin-State Energetics, Spin-Density Profiles, and the Remarkable Performance of the OLYP Functional *J. Chem. Theory Comput.* **2007**, *3*, 689-702; (c) Conradie, J.; Ghosh, A. DFT Calculations on the Spin-Crossover Complex Fe(salen)(NO): A Quest for the Best Functional *J. Phys. Chem. B* **2007**, *111*, 12621-12624.

(25) (a) Haeusermann, U.; Dolg, M.; Stoll, H.; Preuss, H.; Schwerdtfeger, P.; Pitzer, R. M. Accuracy of energy-adjusted quasirelativistic ab initio pseudopotentials *Mol. Phys.* **1993**, *78*, 1211-1224. (b) Kuechle, W.; Dolg, M.; Stoll, H.; Preuss, H. Energy-adjusted pseudopotentials for the actinides. Parameter sets and test calculations for thorium and thorium monoxide *J. Chem. Phys.* **1994**, *100*, 7535-7542. (c) Leininger, T.; Nicklass, A.; Stoll, H.; Dolg, M.; Schwerdtfeger, P. The accuracy of the pseudopotential approximation. II. A comparison of various core sizes for indium pseudopotentials in calculations for spectroscopic constants of InH, InF, and InCl *J. Chem. Phys.* **1996**, *105*, 1052-1059.

(26) (a) Ditchfield, R.; Hehre, W. J.; Pople, J. A. Self-Consistent Molecular-Orbital Methods. IX. An Extended Gaussian-Type Basis for Molecular-Orbital Studies of Organic Molecules *J. Chem. Phys.* **1971**, *54*, 724-728. (b) Hehre, W. J.; Ditchfield, R.; Pople, J. A. Self-Consistent Molecular Orbital Methods. 12. Further extensions of Gaussian-type basis sets for use in molecular-orbital studies of organic-molecules *J. Chem. Phys.* **1972**, *56*, 2257-2261. (c) Hariharan, P. C.; Pople, J. A. Accuracy of AH equilibrium geometries by single determinant molecular-orbital theory *Mol. Phys.* **1974**, *27*, 209-214. (d) Gordon, M.

S. The isomers of silacyclopropane *Chem. Phys. Lett.* **1980**, *76*, 163-168. (e) Hariharan, P. C.; Pople, J. A. Influence of polarization functions on molecular-orbital hydrogenation energies *Theor. Chim. Acta* **1973**, *28*, 213-222.

(27) (a) Peng, C.; Ayala, P. Y.; Schlegel, H. B.; Frisch, M. J. Using redundant internal coordinates to optimize equilibrium geometries and transition states *J. Comp. Chem.* **1996**, *17*, 49-56. (b) Peng, C.; Schlegel, H. B. Combining Synchronous Transit and Quasi-Newton Methods for Finding Transition States *Israel J. Chem.* **1993**, *33*, 449-454.

(28) (a) Carpenter, J. E.; Weinhold, F. Analysis of the geometry of the hydroxymethyl radical by the "different hybrids for different spins" natural bond orbital procedure *J. Mol. Struct. (Theochem)*, **1988,** *169*, 41-62. (b) Carpenter, J. E. Extension of Lewis structure concepts to open-shell and excited-state molecular species *PhD. Thesis*. University of Wisconsin, Madison, WI, **1987**. (c) Foster, J. P.; Weinhold, F. Natural hybrid orbitals *J. Am. Chem. Soc.*, **1980,** *102*, 7211-7218. (d) Reed, A. E.; Weinhold, F. Natural bond orbital analysis of near-Hartree-Fock water dimer *J. Chem. Phys.*, **1983,** *78*, 4066-4073. (e) Reed, A. E.; Weinhold, F. Natural localized molecular orbitals *J. Chem. Phys.*, **1985,** *83*, 1736-1740. (f) Reed, A. E.; Weinstock, R. B.; Weinhold, F. Natural population analysis *J. Chem. Phys.*, **1985,** *83*, 735-746. (g) Reed, A. E.; Curtiss, L. A.; Weinhold, F. Intermolecular interactions from a natural bond orbital, donor-acceptor viewpoint *Chem. Rev.*, **1988,** *88*, 899-926. (h) Weinhold, F.; Carpenter, J. E. *The Structure of Small Molecules and Ions*. Plenum, New York, **1988**; p 227.

(29) *NBO 5.0*. Glendening, E. D.; Badenhoop, J. K.; Reed, A. E.; Carpenter, J. E.; Bohmann, J. A.; Morales, C. M.; Weinhold, F.; Theoretical Chemistry Institute, University of Wisconsin, Madison, **2001**.

(30) Portmann, S.; Lüthi, H. P. MOLEKEL: An Interactive Molecular Graphics Tool *Chimia* **2000**, *54*, 766-770.

(31) Harvey, J. N.; Aschi, M.; Schwarz, H.; Koch, W. The singlet and triplet states of phenyl cation. A hybrid approach for locating minimum energy crossing points between non-interacting potential energy surfaces *Theor. Chem. Accts.* **1998**, *99*, 95-99.

(32) Baboul, A. G.; Schlegel, H. B. Improved Method for Calculating Projected Frequencies along a Reaction Path *J. Chem. Phys.* **1997**, *107*, 9413-9417.